Journal of ELECTRONIC MATERIALS, Vol. 43, No. 7, 2014
DOI: 10.1007/s11664-014-3117-2

Synthesis of Nanosize Quasispherical $MgFe_2O_4$ and Study of Electrochemical Properties as Anode of Lithium Ion Batteries

HAOWEN LIU[1,2,3] and HEFEN LIU[1]

1.—Key Laboratory of Catalysis and Materials Science of the State Ethnic Affairs Commission & Ministry of Education, South-Central University for Nationalities, Wuhan 430074, Hubei, People's Republic of China. 2.—e-mail: liuhwchem@mail.scuec.edu.cn. 3.—e-mail: liuhwchem@hotmail.com

In this work, nanosize $MgFe_2O_4$ spinel with quasispherical shape was prepared as anode material for lithium ion batteries by the hydroxide coprecipitation method. The crystal structure, composition, and morphology of the as-prepared powders were characterized by means of x-ray diffraction (XRD) analysis, x-ray photoelectron spectroscopy, and scanning electron microscopy (SEM), respectively. The XRD and SEM data revealed that the material as-prepared at 900°C was of high crystallinity and quasispherical with diameter of about 100 nm. A reaction mechanism is proposed. The electrochemical properties were evaluated by cyclic voltammetry and galvanostatic charge–discharge studies. The sample calcined at 900°C delivered a higher initial discharge capacity (1200 mAh g^{-1}) and better cyclability. The enhanced electrochemical behavior was ascribed to the nanosize and the better crystallinity of the spherical powder. All the results suggest that nanosize quasispherical $MgFe_2O_4$ is a promising candidate anode material for lithium ion batteries.

Key words: Lithium ion batteries, anode material, $MgFe_2O_4$, hydroxide coprecipitation method

INTRODUCTION

Consumer demand for larger-scale applications such as plug-in hybrid electric vehicles (PHEVs) and electric vehicles (EVs) has led to the development and optimization of lithium ion batteries, in particular the development of anode materials with higher energy and power densities. Currently, most commercial Li ion batteries use carbon graphite (LiC_6) as anode. However, the theoretical capacity of LiC_6 is only 372 mAh g^{-1}, which limits the development of lithium ion batteries. Alternative anode materials include metal ferrite oxide spinels such as $ZnFe_2O_4$, $NiFe_2O_4$, $CuFe_2O_4$, and $CoFe_2O_4$.[1–4]These spinels can react reversibly with lithium ions according to the following reversible reaction: $AFe_2O_4 + 8e^- + 8Li^+ \leftrightarrow A + 2Fe + 4Li_2O$ (A = metal element). Thus, they can provide twice the capacity per unit mass and three times the density, which is very suitable for anodes of lithium ion batteries; For example, Li et al. obtained $NiFe_2O_4$ with a high initial discharge capacity of 1239 mAh g^{-1} by using Ni-Fe^{2+}-Fe^{3+}-layered double hydroxides as the precursor.[5] We have also reported that the initial discharge capacity of nanosize $NiFe_2O_4$ reached 1400 mAh g^{-1}.[2]

Among the ferrite oxide spinels, magnesium ferrite spinel ($MgFe_2O_4$) is known for its low cost, environmental friendliness, and ideal mixed-spinel structure.[6–8] However, use of $MgFe_2O_4$ as anode for lithium ion batteries has been reported only twice in the literature. Lots of work remains to be done. Lee and coworkers[9] obtained a discharge capacity of around 850 mAh g^{-1}. Compared with the theoretical discharge capacity of $MgFe_2O_4$ (1072 mAh g^{-1}), it is necessary to improve its electrochemical performance. Bai and coworkers[10] coated carbon on the surface of $MgFe_2O_4$ to increase its electrical conductivity. However, the electrochemical properties

(Received October 26, 2013; accepted March 8, 2014; published online March 28, 2014)

of bare $MgFe_2O_4$ are not clear. In particular, $MgFe_2O_4$ investigated by the authors is often mixed with iron oxide. Pure $MgFe_2O_4$ must be prepared.

Obviously, particle size and shape play a key role in influencing the material properties. For use as electrodes of lithium ion batteries, spherical powder has many advantages such as high tap density, excellent fluidity, and dispersivity.[11] The hydroxide coprecipitation method has often been used as a major preparation technique to obtain spherical powders.[12] Here, we introduce the hydroxide coprecipitation method to prepare a series of nanosize $MgFe_2O_4$ powders with quasispherical shape. The structure, composition, shape, reaction mechanism, and electrochemical performance of the as-synthesized powders are studied.

EXPERIMENTAL PROCEDURES

In a typical synthesis, 30 mL 0.5 mM $MgSO_4$ and 1.0 mM $FeCl_3{\cdot}6H_2O$ were respectively dripped at the same rate into a beaker filled with 50 mL 4 mM NaOH solution. The stirring speed was 20 revolutions per second. The pH value was adjusted to 10 using $NH_3{\cdot}H_2O$, then the mixtures were kept for 6 h at 45°C under stirring. After the reaction, the mixture was filtered and washed several times with distilled water, then heated for 8 h at high temperature in a muffle furnace, followed by air cooling to room temperature to obtain the final powder.

Phase identification of the product was carried out by x-ray diffraction (XRD) analysis using a D8 Advance diffractometer (Bruker, Saarbrücken, Germany) with Cu K_α radiation (λ = 1.5406 Å) at current of 40 mA and potential of 40 kV. The XRD patterns were collected in steps of 0.02° in the range of $10° \le 2\theta \le 70°$ with constant counting time of 0.1 s per step at room temperature, and Rietveld analysis was conducted using TOPS 3 refinement software (Bruker, Saarbrücken, Germany). The morphology was investigated by field-emission scanning electron microscope (SEM; JEOL Ltd., Kyoto, Japan). Tap densities were determined using a VanKel tap density measuring device (Hosokawa Micron Co., Hong Kong, China) in a 25-mL graduated cylinder with 1000 taps. The x-ray photoelectron spectroscopy (XPS) patterns of the products were measured using an x-ray photoelectron spectrometer (XPS; Thermo Co., MA) with a monochromatic Al K_α light source. Each spectrum was calibrated using the C 1*s* binding energy (BE) at 284.6 eV. Simulated cells were assembled using lithium foil as the counter and reference electrode in an argon-filled glovebox (Mbrun Co., Munich, Germany). The anode materials were the as-prepared powders mixed with 12% acetylene black and 8% polytetrafluoroethylene (PTFE). The electrolyte was 1 M $LiPF_6$ in a 1:1 mixture of ethylene carbonate/diethyl carbonate, and the separator was Celgard 2300. Cyclic voltammetry (CV) was performed using a CHI660A electrochemical workstation (CH Instrument Co., Shanghai, China). Charge–discharge cycles were performed between 0.0 V and 3.0 V with current of 0.2 mA cm^{-2}. All electrical measurements were carried out using a battery testing system (BTS-5 V/10 mA; Neware technology, Co., Shanghai, China) at room temperature.

RESULTS AND DISCUSSION

Figure 1 shows the XRD patterns of the powders calcined for 8 h at different temperatures. There are two broad peaks at 2θ values of 35.4° and 62.2° for the 350°C sample, indicating that it was a nearly amorphous phase. For the 600°C powder, the main peaks of $MgFe_2O_4$ powder can be seen. However, some peaks (marked by circles) relating to impurity phase appear at 24.4°, 48.1°, and 63°. This result is consistent with Ref. 10. After 900°C, these impurity peaks disappear. Other diffraction peaks are in good agreement with single-phase $MgFe_2O_4$ (JCPDS card no. 73-2410), indicating that $MgFe_2O_4$ begins to form at this temperature. A schematic diagram of the $MgFe_2O_4$ spinel structure is shown in Fig. 2, where bivalent Mg ions occupy the tetrahedral 8a sites, trivalent Fe ions occupy the octahedral 16d sites, and oxygen ions occupy the 32e sites. The strong and narrow peaks in the obtained XRD pattern show that the material is well crystallized. Refinement was completed using TOPS 3 software with a convincing R_{wp} value of 7.5. The lattice parameter of the 900°C sample was calculated to be 8.369 Å, in good accordance with the database value of 8.376 Å (JCPDS card no. 73-2410), and the average crystalline size was calculated from the (222) peak to be 98 nm using the Scherrer equation[2] $D = \frac{0.89\lambda}{\beta \cos\theta}$,, where β is the full-width at half-maximum of the (222) peak, θ is the angle of reflection, and λ = 1.54056 Å.

Figure 3 shows SEM images of the precursor calcined for 8 h at above 700°C. The particles are

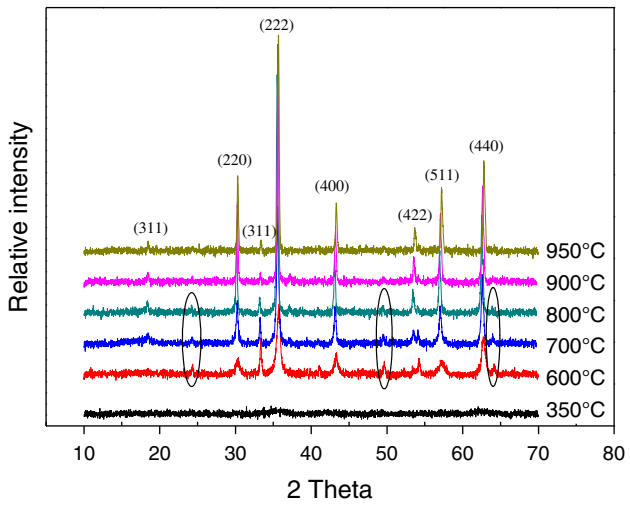

Fig. 1. XRD patterns of $MgFe_2O_4$ powders calcined at different temperatures.

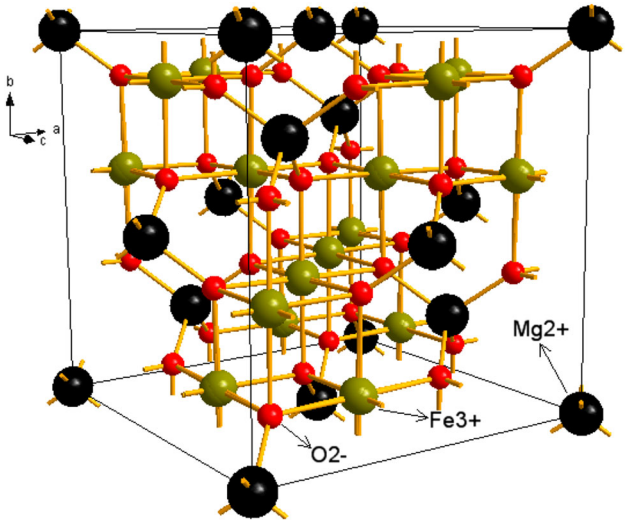

Fig. 2. Schematic of the $MgFe_2O_4$ unit cell.

quasispherical, and the particle size increases significantly with increasing heat-treatment temperature. The average diameter of the primary particles increased from about 30 nm in the 700°C sample to 100 nm in the 900°C sample. Especially for the 950°C powder, the particle size increased abruptly from 100 nm to 500 nm, an increase of nearly 500%. The tap densities of the obtained precursors were about 1.24 g cm^{-3}, 1.53 g cm^{-3}, 1.81 g cm^{-3}, and 2.52 g cm^{-3} for the 700°C, 800°C, 900°C, and 950°C samples, respectively. In general, spherical particles exhibit fewer vacancies and excellent fluidity, leading to higher tap density values than for powder composed of irregular particles.[13] Mg and Fe prefer different pH values to precipitate. When the pH is not adjusted properly, particles of other shapes are obtained. So the chelating metal ion $[M(NH_3)_x]$ concentration is the key factor to obtain particles of spherical shape. According to the experimental process, the following reaction mechanism can be proposed:

$$Mg^{2+} + nNH_3 \cdot H_2O = Mg(NH_3)_n^{2+} + nH_2O \quad (1)$$

$$Mg(NH_3)_n^{2+} + 2OH^- + nH_2O = Mg(OH)_2 + nNH_3 \cdot H_2O \quad (2)$$

$$Mg(OH)_2 = MgO + H_2O \quad (3)$$

$$Fe^{2+} + mNH_3 \cdot H_2O = Fe(NH_3)_m^{2+} + mH_2O \quad (4)$$

$$Fe(NH_3)_m^{2+} + 2OH^- + mH_2O = Fe(OH)_3 + mNH_3 \cdot H_2O \quad (5)$$

$$Fe(OH)_3 = Fe_2O_3 + H_2O \quad (6)$$

$$MgO + Fe_2O_3 = MgFe_2O_4 \quad (7)$$

$$Mg(OH)_2 + 2Fe(OH)_3 = MgFe_2O_4 + 4H_2O \quad (8)$$

Figure 4 illustrates the hypothesized evolution of the quasispherical $MgFe_2O_4$. At the beginning of the reaction, fine particles of metal oxides are formed and then combine with each other to form nanocrystalline magnesium ferrite oxide particles. The particles grow gradually and develop a smooth and uniform quasispherical morphology without further agglomeration.

XPS analysis was used to investigate the chemical composition and states of $MgFe_2O_4$ calcined at 900°C. As shown in the XPS survey spectrum in Fig. 5, this sample consisted of only magnesium, iron, carbon, and oxygen elements. The BE scales are referenced to the C 1*s* BE of 284.6 eV. The BE peaks located at 48.47 eV, 710.2 eV, and 529.7 eV correspond to Mg 2*p*, Fe $2p_{3/2}$, and O 1*s*, respectively. All the values are similar to the reported values except for nitrogen peaks.[10]

CV was carried out for the electrode made from the 900°C sample. Li metal was used for the reference and working electrode. The scan rate was 0.1 mV s^{-1}, and the potential was in the range of 0.05 V to 3.00 V. The first two cycles are shown in Fig. 6. There is a broad peak centered at 0.68 V in the first cathodic process, which should be ascribed to reduction of MgO and Fe_2O_3 to metallic Mg and Fe. In the second cycle, this peak shifts to about 0.97 V, which could be ascribed to polarization of the electrode materials in the first cycle. A small peak centered at 1.34 V can be seen. Guo et al.[14] attributed it to incomplete reduction of Fe^{3+} to Fe^{2+}. However, He et al.[15] believed it might be related to the reduction of the irreversible reaction with the electrolyte. Further investigation is underway. During the anodic process, two peaks are present at 1.50 V and 1.75 V, which are associated with oxidation of metallic Mg and Fe to Mg^{2+} and Fe^{3+}, respectively. In the subsequent charging process, these two anodic peaks shift to 1.68 V and 1.85 V, which also might be ascribed to polarization of the electrode materials in the first cycle.[16] Compared with the first charge–discharge process, the decrease of the redox peak intensity and the integrated area in the second cycle indicates that the capacity is decreased.

Charge–discharge tests were carried out with the synthesized $MgFe_2O_4$ samples as the anodic material. The current was 0.2 mA cm^{-2}, and the voltage was in the range from 0.0 V to 3.0 V. Figure 7 shows the first two charge–discharge

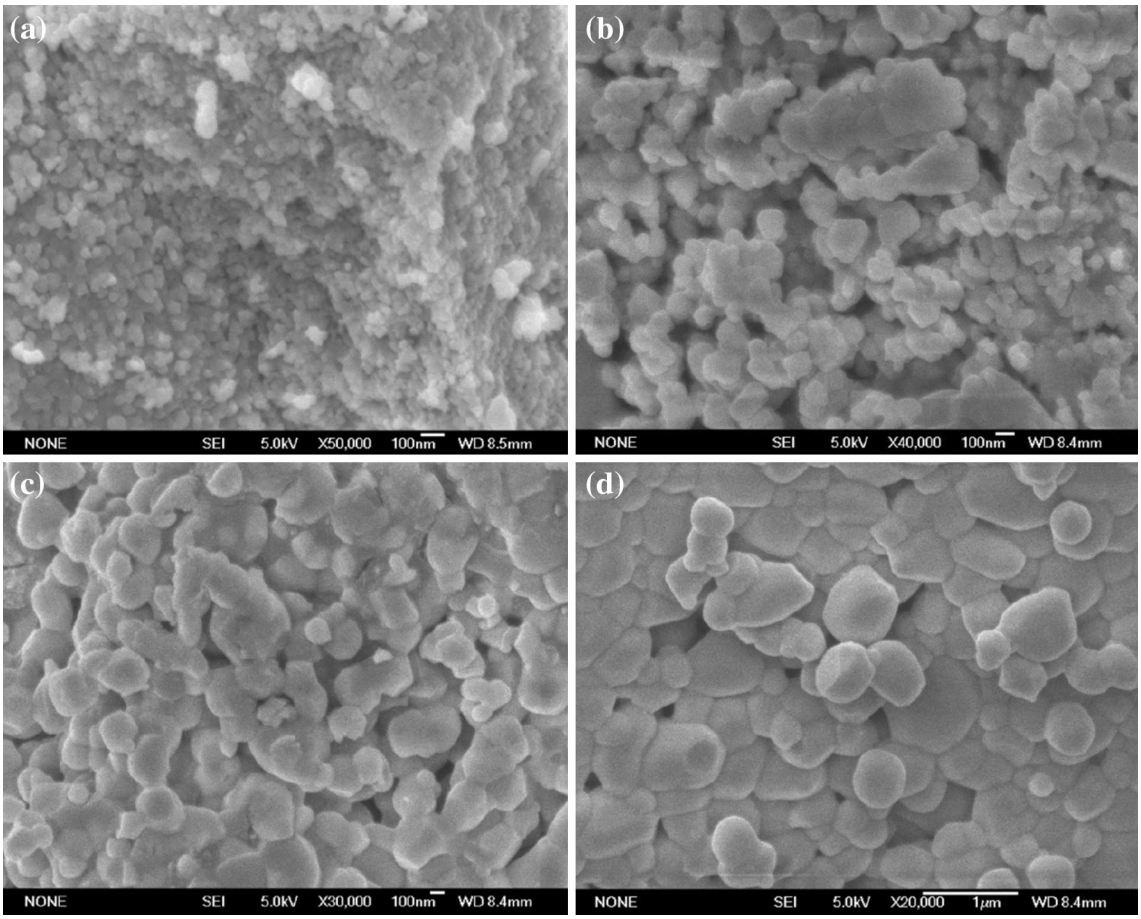

Fig. 3. SEM images of powders obtained at deferent temperatures: (a) 700°C, (b) 800°C, (c) 900°C, and (d) 950°C.

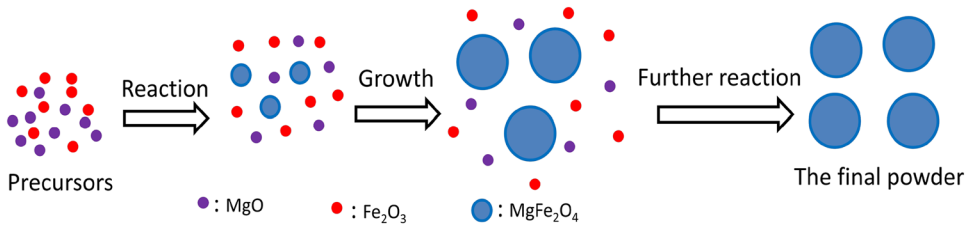

Fig. 4. Illustration of the formation procedure of quasispherical $MgFe_2O_4$.

curves for the 900°C powder. The charge–discharge capacity was 1243 mAh g^{-1}/1200 mAh g^{-1} and 1080 mAh g^{-1}/1070 mAh g^{-1}, respectively. There are two potential plateaus around 1.0 V and 0.75 V in the discharge curves, which can be attributed to the corresponding reductions of Mg^{2+} to Mg and Fe^{3+} to Fe. The plateaus in the charge curves may be related to metal oxide reactions. According to previous studies,[9,17] the entire electrochemical process can be proposed as follows:

$$MgFe_2O_4 + 8Li^+ + 8e^- \rightarrow Mg + 2Fe + 4Li_2O \quad (9)$$

$$4Li_2O + Mg + 2Fe \leftrightarrow MgO + Fe_2O_3 + 8Li \quad (10)$$

Figure 8 shows the cycling properties of the synthesized $MgFe_2O_4$ at 0.2 mA cm^{-2} in the range from 0.0 V to 3.0 V. The initial discharge capacity was 1380 mAh g^{-1}, 1301 mAh g^{-1}, 1200 mAh g^{-1}, and 978 mAh g^{-1} for the powders prepared at 700°C, 800°C, 900°C, and 950°C, respectively. The values decrease with increasing calcination temperature, which may be attributed to the particle size increase. After several cycles, the impurity phase in the powders prepared at 700°C and 800°C leads to serious capacity loss. The discharge capacities decrease rapidly during the first six cycles for the samples sintered at 900°C and 950°C. This damage is due to volume changes of the active sites during Li insertion and deinsertion. Large volume

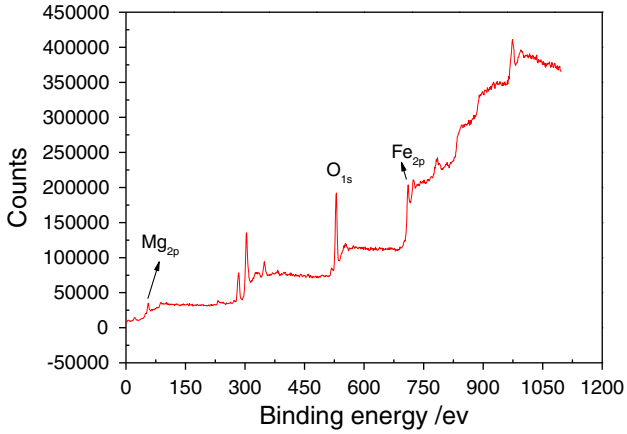

Fig. 5. XPS survey spectrum of $MgFe_2O_4$ annealed at 900°C.

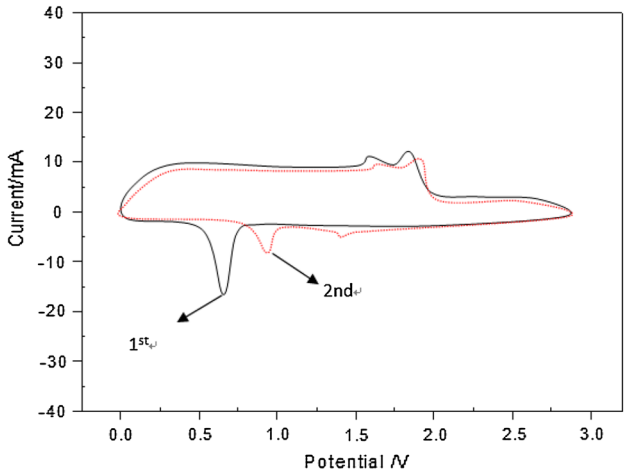

Fig. 6. The first two CV cycles of $MgFe_2O_4$ prepared at 900°C measured at scan rate of 0.1 mV s^{-1} between 0.05 V and 3.00 V.

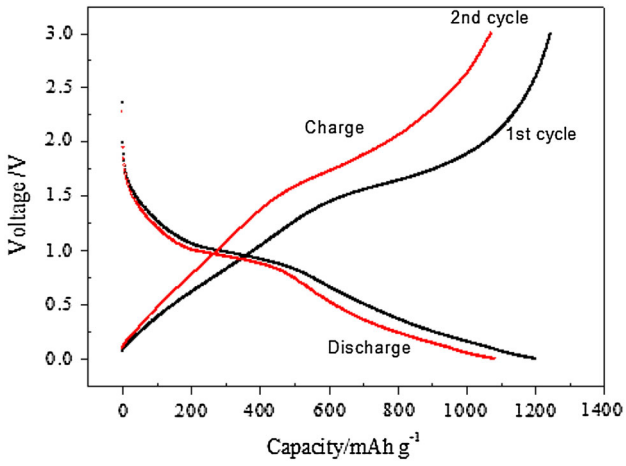

Fig. 7. The first two charge–discharge curves of the sample prepared at 900°C as anode at 0.2 mA cm^{-2} in the range 0.0 V to 3.0 V.

expansion occurs when Li intercalates into $MgFe_2O_4$, and in the reverse deinsertion process there is a large volume shrinkage, which limits the

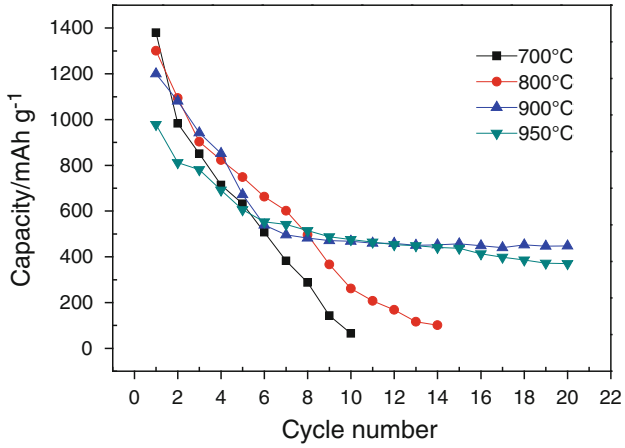

Fig. 8. Cycling properties of the obtained samples at 0.2 mA cm^{-2} in the range 0.0 V to 3.0 V.

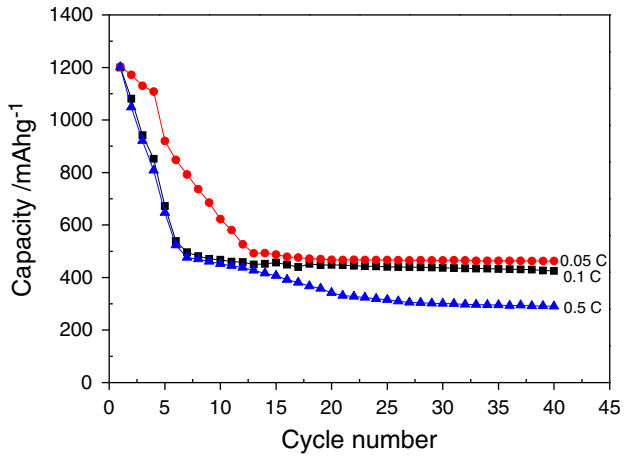

Fig. 9. Discharge rate capacity versus cycles of the sample as-prepared at 900°C in the range 0.0 V to 3.0 V (1 C = 200 mAh g^{-1}).

battery lifetime. In addition, the irreversible capacity can be related to decomposition of the electrolyte and the formation of an organic layer on the surface of the particles when the cell potential approaches 0 V.[1] This large capacity loss is the major drawback of these potential candidates for negative electrodes of lithium ion batteries.[9,18] After six cycles, the discharge capacity of the powder prepared at 900°C decayed more slowly, stabilizing at about 460 mAh g^{-1} and 448 mAh g^{-1} after 10 and 20 cycles, respectively. However, the discharge capacity decrease was 79.73% after 10 cycles in Ref. 9. It is generally known that quasispherical shape with larger surface can improve the capacity and charge–discharge cyclability. Furthermore, nanosize can also give a shorter diffusion length for lithium ions and accommodate easily the structural strain associated with the electrochemical reaction.[1,19] Recently, Aifantis et al.[20] reported that smaller particle sizes resulted in greater mechanical and hence electrochemical stability. Compared with the 900°C powder, the 950°C powder showed worse

cyclability, which may be ascribed to the large size and low conductivity. The rate capacity of the $MgFe_2O_4$ prepared at 900°C was measured in the range from 0.0 V to 3.0 V and is shown in Fig. 9. The discharge capacity reaches 463 mAh g^{-1}, 425 mAh g^{-1}, and 290 mAh g^{-1} after 40 cycles at 0.05 C, 0.1 C, and 0.5 C, respectively. The capacity retention is 38.5%, 35.4%, and 24.1%, respectively. From these data, it can be seen that $MgFe_2O_4$ shows better discharge capacity at lower current density.

CONCLUSIONS

Nanosize $MgFe_2O_4$ spinel with quasispherical shape was successfully synthesized by the hydroxide coprecipitation method at different calcination temperatures. From the XRD data, we conclude that 900°C is the optimal calcination temperature in this experiment. As the anode material of lithium ion batteries, the highest initial discharge capacity was found for $MgFe_2O_4$ prepared at 900°C, being 1200 mAh g^{-1} at 0.2 mA g^{-1} in the range from 0.0 V to 3.0 V. Better capacity retention was achieved. The results presented herein prove that it could be possible to replace LiC_6 anode with magnesium ferrite spinel, consisting only of elements that are abundant in the Earth's crust, for the development of large-scale applications in present lithium batteries.

REFERENCES

1. F. Mueller, D. Bresser, E. Paillard, M. Winter, and S. Passerini, *J. Power Sources* 236, 87 (2013).
2. H. Liu, H. Zhu, and H. Yang, *Mater. Res. Bull.* 48, 1587 (2013).
3. L. Jin, Y. Qiu, H. Deng, W. Li, H. Li, and S. Yang, *Electrochim. Acta* 56, 9127 (2011).
4. Z.H. Li, T.P. Zhao, X.Y. Zhan, D.S. Gao, Q.Z. Xiao, and G.T. Lei, *Electrochim. Acta* 55, 4594 (2010).
5. H. Zhao, Z. Zheng, K.W. Wong, S. Wang, B. Huang, and D. Li, *Electrochem. Commun.* 9, 2606 (2007).
6. Y. Shen, Y. Wu, X. Li, Q. Zhao, and Y. Hou, *Mater. Lett.* 96, 85 (2013).
7. J.Y. Patil, I.S. Mulla, and S.S. Suryavanshi, *Mater. Res. Bull.* 48, 778 (2013).
8. V.M. Khot, A.B. Salunkhe, N.D. Thorat, R.S. Ningthoujam, and S.H. Pawar, *Dalton Trans.* 42, 1249 (2013).
9. N. Sivakumar, S.R.P. Gnanakan, K. Karthikeyan, S. Amaresh, W.S. Yoon, G.J. Parkd, and Y.S. Lee, *J. Alloys Compd.* 509, 7038 (2011).
10. C. Gong, Y. Bai, Y. Qi, N. Lun, and J. Feng, *Electrochim. Acta* 90, 119 (2013).
11. M.-H. Lee, Y.-J. Kang, S.-T. Myung, and Y.-K. Sun, *Electrochim. Acta* 50, 939 (2004).
12. T. Wang, Z. Liu, L. Fan, Y. Han, and X. Tang, *Powder Technol.* 187, 124 (2008).
13. J.R. Ying, C.Y. Jiang, and C.R. Wan, *J. Power Sources* 29, 264 (2004).
14. X.W. Guo, X. Lu, X.P. Fang, Y. Mao, Z.Y. Wang, L.Q. Chen, X.W. Xu, H. Yang, and Y.N. Liu, *Electrochem. Commun.* 12, 847 (2010).
15. Y. He, L. Huang, J.S. Cai, X.M. Zheng, and S.G. Sun, *Electrochim. Acta* 55, 1140 (2010).
16. Y. Deng, Q. Zhang, S. Tang, L. Zhang, S. Deng, Z. Shi, and G. Chen, *Chem. Commun.* 47, 6828 (2011).
17. X. Yang, X. Wang, and Z. Zhang, *J. Cryst. Growth* 277, 467 (2005).
18. R. Alcantara, M. Jaraba, P. Lavela, J.L. Tirado, J.C. Jumas, and J.O. Fourcade, *Electrochem. Commun.* 5, 16 (2003).
19. Y.S. Lee, Y.K. Sun, K. Adachi, and M. Yoshio, *Electrochim. Acta* 48, 1031 (2003).
20. K.E. Aifantis, T. Huang, S.A. Hackney, T. Sarakonsri, and A. Yu, *J. Power Sources* 197, 246 (2012).